

EXPERIMENTAL AND NUMERICAL ANALYSIS OF FRETTING FATIGUE CRACK INITIATION IN DOVETAIL JOINT FOR AERO ENGINE COMPRESSOR

*Z.U. HASSAN, M.M.I. HAMMOUDA, S. KHUSHNOOD, K. AKHTAR¹, M. JAHANZEB and A. MALIK

University of Engineering & Technology, Taxila, Pakistan

¹National University of Sciences and Technology (NUST), Islamabad, Pakistan

(Received May 15, 2012 and accepted in revised form December 13, 2012)

This paper presents the development of a unique, safe and flexible fretting fatigue experimental test rig for analysis of fretting fatigue crack initiation in dovetail joint of aero-engine compressor. The testing rig is capable for revolving the specimen disc and blades in the range of 0 ~ 20,000 rpm and reverse back to zero rpm in small increments. Different experimental test rigs already designed by various researchers were evaluated on the basis of their capability. This conceptual design test rig is unique addition in the fretting fatigue testing field and is helpful for testing of different type of joints and materials. The experiments for bakelite and structural steel have been performed and conclude that the edge of common surface near the dovetail notch base is the fretting fatigue failure of the disc. The modeling and simulation has been carried out using commercially available software. It is found in each iteration analysis irrespective of thickness and material of the disc, fillet is the weakest portion in the model.

Keywords: Fretting fatigue, Test rig, Dovetail joint, Experimental approach, Aero engine

1. Introduction

Transportation of various equipments is done by using aero planes, vehicles and robots. The structural integrity of the main parts of the carrying aero-plane must be ensured, inspected and analyzed to avoid any damage to human life as well as loaded equipments. Fretting fatigue is responsible to damage the attachment of structural components i.e., disc and blades. This mechanism is addressed through experimental investigation and various numerical approaches have been adopted to find the approximate solutions. The fretting fatigue phenomenon is a serious threat for mechanical components and the service they performed apart of engineering structures. It includes air and space craft components, automobiles sub-assemblies and various diversified electrical and manufacturing equipment etc. Dovetail joints are used to fixed the blades on the disc for the fan assembly and in the low pressure stage of rotating compressors in turbine used for air craft propulsion. Conner et al. [1] found fretting fatigue phenomenon in these joints. Eden and Rose [2] identified fretting fatigue and observed production of iron oxide on the contact

surfaces of a fatigued specimen. Tomilson [3] carried out its first scientific study on the phenomenon and found that it took place due to the tangential motion between surfaces which are in contact with each other. Nowell [4] worked on fretting crack initiation effects on fatigue life on Aluminum 4% Cu alloy. He pointed out the performance effects of fretting by many factors including microstructure and environmental variables. Shinde and Hoepfner [5] have experimentally concluded that initiation and propagation of cracks responded to different factors. Alfredsson and Cadario [6] through their investigations concluded that in case of long crack propagation life in fretting fatigue has practically a comparatively low proportion against total part life whereas Conner et al. [7] found that short crack stage has been given comparatively less concentration till date. Nowell and Dini [8] concluded that a quantitative accurate model of this phenomenon has not yet completely developed. Ramakrishna et al. [9] explained that large broken particles of material filled the mouth of the notch, ultimately one or two cracks appeared in dominated position to propagate and

* Corresponding author : zaheerpof@yahoo.com

Fouvry et al. [10] also developed experimental methodologies to define crack nucleation boundary under various laboratory conditions. Hutson et al. [11] inferred that crack nucleation is defined in terms of crack observed which is ranging from 0.1 to 0.5 mm depending upon the capacity of experimental testing system.

Numerous attempts were made to predict the performance of components under fretting fatigue loadings to predict the crack initiation site, direction and life prediction under certain set of conditions. The parameters defined by numerous researchers for fretting fatigue performance can be mainly divided into special parameters approaches, critical plane approaches and fracture mechanics based approaches. Some of these parameters are used for crack initiation while some of the parameters are used for both crack initiation and life prediction.

Critical planes developed from a physical interpretation of fatigue process whereby cracks were observed to initiate and grow on certain special material planes. In this approach, stresses and strains during the loading cycle are determined for various planes at the same special position in the component. These empirical parameters also provide the direction of early crack growth of crack and a measure of the multiaxial fatigue damage that can be correlated with simple uniaxial fatigue data to initiation life. The commonly used critical plane parameters (CPP) are:- Modified Smith-Watson Topper (SWT) [12], Modified Shear Stress Range (MSSR) [13] and Findley (F) [14].

Hammouda et al. [15] carried out two dimensional finite element analysis to evaluate the probable site of fretting fatigue cracking in disc and blades fixed in dovetail joint in aero engine compressor. He concluded that edge of common surface near the dovetail notch base is the site of initiation of fatigue failure of the disc. Malay et al. [16] carried out analysis of dovetail joints through three dimensional numerical simulations and revealed that large stresses variation through disc thickness which cannot be predicted in two dimensional analyses. Kaliyaperumal et al. [17] investigated and observed that preloading at the dovetail interface reduces the peak contact pressure developed due to bulk loading upto 35 %. Tiago et al. [18] analyzed gas turbine blades and concluded that max stress occurred in case five and it shows that angle 40 degree is not appropriate.

Different experimental testing systems have been used to study fretting fatigue phenomenon. Most of them include experimental testing systems with simple geometries for which analytic solutions exist for contact stress distribution. Some of the most popular and widely used experimental testing systems with reference to fretting fatigue research are bridge type, cylindrical type and structure dependent type. Corner and Nicholas introduced a fretting fatigue fixture which was further modified by Patrick and Golden [19] for turbine engine material at elevated temperature. Borms et al. [20] introduced test rig with improved conceptual design. Pauw et al. [21] reviewed all the state of the art fretting fatigue test rigs being used on the basis of their properties and concluded that still have imperfection.

The main objective of this research work is to design and develop a new flexible, safe and improved experimental test rig to investigate fretting fatigue crack initiation experimentally in dovetail joints disc and blade of aero engine compressors and commercially available software has been verified by the experimental performance in the model.

2. Experimentation

To investigate the crack initiation experimentally in the dovetail joint of aero engine compressor, a new testing rig was designed and developed. The detail is as under.

2.1 Design and Development of Experimental Test Rig

Experimental test rig capable of simulating incipient fretting fatigue failure was designed with following consideration.

- Revolving the specimen, disc and blades in a sine wave pattern or mark which is the actual simulation i.e. acceleration and deceleration of aero engine compressors.
- The testing rig has a capability of revolving specimen continuously from zero to twenty thousand and reverse back from twenty thousand to zero rpm.
- Easy fixing of the specimen (disc and blades) on the shaft of main motor.

The extreme safety was desirable for revolving the specimen, disc and blades up to twenty

thousand rpm which is very high speed. The photograph of testing rig and exploded view of testing fixture is given in Figures 1 and 2 respectively. Different mechanical parts used in the testing fixture and control the speed of the testing rig is given in Figures 3 and 4 respectively.



Figure 1. Experimental testing rig showing (1) the assembly testing fixture and (2) speed control system of the rig.

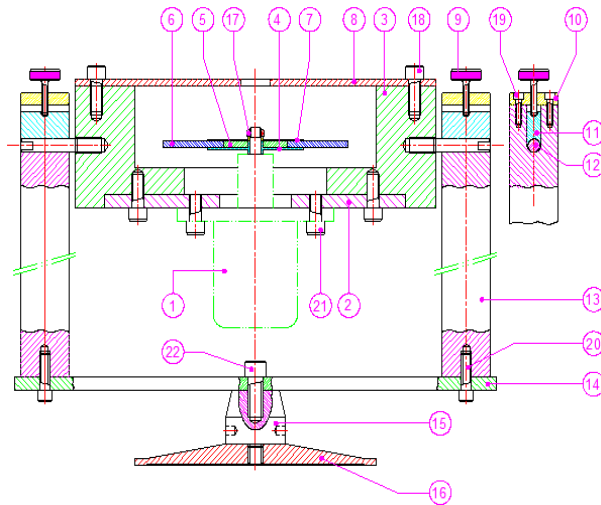


Figure 2. The exploded view of test fixture.

| | | |
|-------------------------|----------------------------|--------------------|
| 1. Main motor | 2. Mainmotor holding plate | 3. Safety guard |
| 4. Lower holding plate | 5. Disc | 6. Blades |
| 7. Upper holding plate | 8. Frount safety plate | 9. Tighting knobs |
| 10. Knobe holding plate | 11. Gripping piece | 12. Revolving pins |
| 13. Pillers | 14. Base plate | 15. Rached |
| 16. Base | 17. Nut | 18. ~22 Std. Screw |



Figure 3. Detail of mechanical parts of test fixture.

| | | |
|-------------------------|----------------------------|--------------------|
| 1. Main motor | 2. Mainmotor holding plate | 3. Safety guard |
| 4. Lower holding plate | 5. Disc | 6. Blades |
| 7. Upper holding plate | 8. Frount safety plate | 9. Tighting knobs |
| 10. Knobe holding plate | 11. Gripping piece | 12. Revolving pins |
| 13. Pillers | 14. Base plate | 15. Rached |
| 16. Base | | |

2.2. Working of Test Rig

Blades were fixed diametrically opposite on disc. The specimen was fixed on the shaft of the main motor directly with the help of upper and lower holding plates. The main motor was fixed on the motor holding plate which was further attached with the safety guard and stand with the help of the pin hinges. This unit is subsequently mounted on the base through ratchet. The safety cover plate is fixed on the safety guard with the help of nuts and bolts.

2.3. Experimental Blades and Disc Model

The dimensions of specimen used in the experimentation are given in Figures 5, 6 and 7. The dovetail joint is symmetric about its central axis. The distance between disc and blade assembly is 1.35 mm. Disc and blades notch base radius is 5 mm and 4 mm respectively. Both the contact surfaces constitute angle of 20° with central axis. The two sectors opposite to each other have been selected to carry out testing.

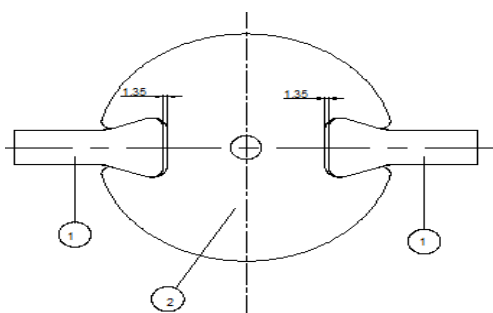


Figure 5. Assembly of two sectors of disc and blades in dovetail joints.

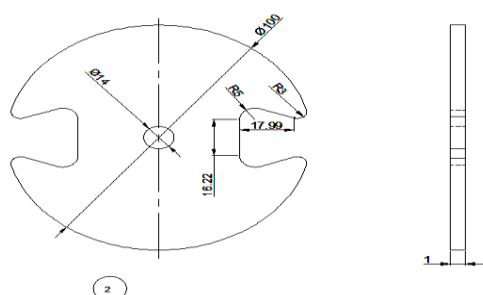


Figure 6. Drawing and dimensions of the disc.

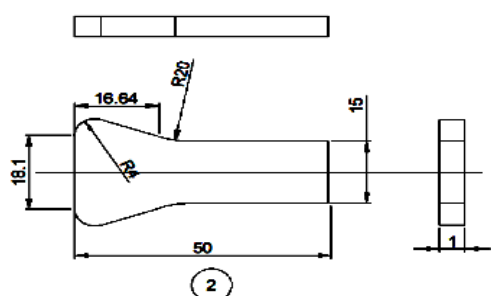


Figure 7. Drawing and dimensions of blades.

2.4 Simulated Loading Cycle

A typical loading cycle consists of acceleration, and deceleration loading. In the present study, the dovetail joint is analyzed during the normal loading cycle of a typical aero engine compressor.

The first phase corresponds to the starting of the engine of an aero engine. During this phase, the aero engine is assumed to be stationary and the engine reaches its maximum speed. Due to increase in speed while the disc is rotating in clockwise direction, the blade tends to move radially outwards. Thus it exerts a force on the disc which is symmetric on both contact surfaces.

The second phase is the deceleration which simulates the stopping of engine. During

deceleration phase, the aero engine is at rest and the engine is stopped by gradually decreasing its speed. Thus acceleration and deceleration loading phases simulate the takeoff and landing of an aero plane. In the present analysis, one acceleration and deceleration cycles have been simulated. However, the simulation could be repeated for more cycles if so desired.

2.5 Running Trend of Testing System – with and without Specimen

To evaluate the experimental test rig performance with and without specimen, same was revolved from 0~20000 rpm with the help of three types of timers i.e. to control “start up time”, “stay time” and “apparatus setup time”. Experimental test rig working was found to be successful. Speed at all the steps was recorded using tachometer. Running trend of experimental test rig with and without specimen is given in Tables 1 and 2 whereas trend depicted graphically in Figures 8 and 9 respectively.

Table 1. Data collected without specimen

| No. | Step Time (Seconds) | Speed (RPM) | No. | Step Time (Seconds) | Speed (RPM) |
|-----|---------------------|-------------|-----|---------------------|-------------|
| 1 | 0.5 | 0 | 32 | 0.5 | 0 |
| 2 | 0.5 | 83 | 33 | 0.5 | 3600 |
| 3 | 0.5 | 1000 | 34 | 0.5 | 6000 |
| 4 | 0.5 | 3400 | 35 | 0.5 | 8300 |
| 5 | 0.5 | 6400 | 36 | 0.5 | 10600 |
| 6 | 0.5 | 8800 | 37 | 0.5 | 12500 |
| 7 | 0.5 | 11200 | 38 | 0.5 | 14000 |
| 8 | 0.5 | 12900 | 39 | 0.5 | 15200 |
| 9 | 0.5 | 14400 | 40 | 0.5 | 16900 |
| 10 | 0.5 | 15600 | 41 | 0.5 | 18400 |
| 11 | 0.5 | 17000 | 42 | 0.5 | 19600 |
| 12 | 0.5 | 18600 | 43 | 0.5 | 20800 |
| 13 | 0.5 | 19900 | 44 | 0.5 | 22000 |
| 14 | 0.5 | 21300 | 45 | 0.5 | 22000 |
| 15 | 0.5 | 22000 | 46 | 0.5 | 22000 |
| 16 | 0.5 | 22000 | 47 | 0.5 | 21700 |
| 17 | 0.5 | 22000 | 48 | 0.5 | 20700 |
| 18 | 0.5 | 21600 | 49 | 0.5 | 19400 |
| 19 | 0.5 | 21600 | 50 | 0.5 | 18000 |
| 20 | 0.5 | 20300 | 51 | 0.5 | 16400 |
| 21 | 0.5 | 19000 | 52 | 0.5 | 14900 |
| 22 | 0.5 | 17600 | 53 | 0.5 | 13200 |
| 23 | 0.5 | 16000 | 54 | 0.5 | 11900 |
| 24 | 0.5 | 14400 | 55 | 0.5 | 9900 |
| 25 | 0.5 | 13000 | 56 | 0.5 | 4200 |
| 26 | 0.5 | 12000 | 57 | 0.5 | 3800 |
| 27 | 0.5 | 11000 | 58 | 0.5 | 2000 |
| 28 | 0.5 | 10000 | 59 | 0.5 | 0 |
| 29 | 0.5 | 9000 | | | |
| 30 | 0.5 | 6000 | | | |
| 31 | 0.5 | 3300 | | | |

Table 2. Data collected with specimen

| No. | Step Time (sec.) | Speed (RPM) | No. | Step Time (sec.) | Speed (RPM) |
|-----|------------------|-------------|-----|------------------|-------------|
| 1 | 0.5 | 0 | 37 | 0.5 | 9400 |
| 2 | 0.5 | 500 | 38 | 0.5 | 8400 |
| 3 | 0.5 | 2000 | 39 | 0.5 | 7400 |
| 4 | 0.5 | 4200 | 40 | 0.5 | 6200 |
| 5 | 0.5 | 5600 | 41 | 0.5 | 5200 |
| 6 | 0.5 | 6600 | 42 | 0.5 | 4000 |
| 7 | 0.5 | 7600 | 43 | 0.5 | 2200 |
| 8 | 0.5 | 8400 | 44 | 0.5 | 400 |
| 9 | 0.5 | 9300 | 45 | 0.5 | 0 |
| 10 | 0.5 | 10000 | 46 | 0.5 | 1700 |
| 11 | 0.5 | 10800 | 47 | 0.5 | 2600 |
| 12 | 0.5 | 11300 | 48 | 0.5 | 3600 |
| 13 | 0.5 | 12100 | 49 | 0.5 | 5000 |
| 14 | 0.5 | 12500 | 50 | 0.5 | 5800 |
| 15 | 0.5 | 13500 | 51 | 0.5 | 6500 |
| 16 | 0.5 | 14200 | 52 | 0.5 | 7400 |
| 17 | 0.5 | 14500 | 53 | 0.5 | 8200 |
| 18 | 0.5 | 15500 | 54 | 0.5 | 8600 |
| 19 | 0.5 | 15700 | 55 | 0.5 | 9500 |
| 20 | 0.5 | 16400 | 56 | 0.5 | 10000 |
| 21 | 0.5 | 17000 | 57 | 0.5 | 10500 |
| 22 | 0.5 | 18000 | 58 | 0.5 | 11400 |
| 23 | 0.5 | 18000 | 59 | 0.5 | 12100 |
| 24 | 0.5 | 17000 | 60 | 0.5 | 12500 |
| 25 | 0.5 | 16400 | 61 | 0.5 | 13100 |
| 26 | 0.5 | 16000 | 62 | 0.5 | 13600 |
| 27 | 0.5 | 16000 | 63 | 0.5 | 14200 |
| 28 | 0.5 | 15800 | 64 | 0.5 | 14500 |
| 29 | 0.5 | 14400 | 65 | 0.5 | 15400 |
| 30 | 0.5 | 14400 | 66 | 0.5 | 16000 |
| 31 | 0.5 | 13800 | 67 | 0.5 | 16500 |
| 32 | 0.5 | 13500 | 68 | 0.5 | 16600 |
| 33 | 0.5 | 12800 | 69 | 0.5 | 17000 |
| 34 | 0.5 | 12000 | 70 | 0.5 | 17100 |
| 35 | 0.5 | 11200 | 71 | 0.5 | 18600 |
| 36 | 0.5 | 10300 | | | |

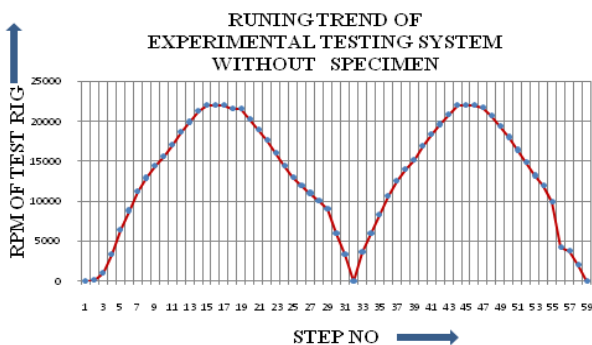


Figure 8. Running trend of experimental test rig without specimen.

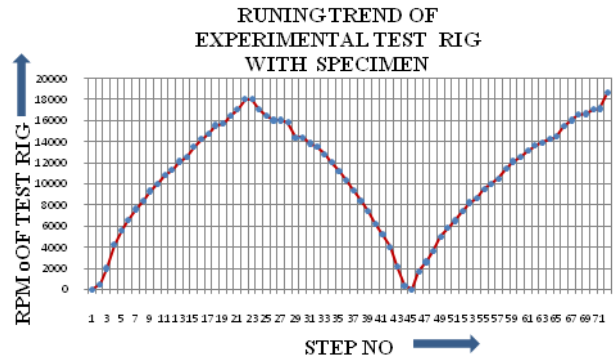


Figure 9. Running trend of experimental test rig with specimen.

2.6. Testing

The specimen was mounted on the spindle of main motor and testing was carried out from 0–20000 rpm. 100 cycles were completed prior to stopping the testing system. The specimen was critically examined and observed no crack on any side of the disc as well as on the blades. However, black powder was found on the sliding surfaces as shown in photograph shown in Figure 10 of the blades and disc known as oxides/debris which is one of the indications of crack initiation which has already been investigated by many researchers.

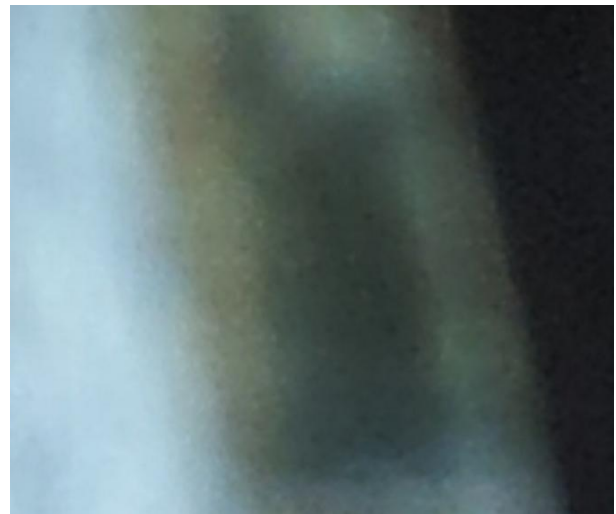


Figure 10. Contact surface of the plate after 100 cycle fretting test stopped contour marked with white line is shown with black powder on the plate surface.

A new specimen, disc and blades were manufactured from the bakelite material on CNC milling machine having identical dimensions to compare the performance. Experiment was carried

out and after 100 cycles specimen was removed after critically examination it showed no crack or damage in the disc or blades and remained intact without any change. After that disc made of bakelite material whereas blades made of structural steel was used and with this combination testing was carried out by starting from zero rpm and when it reached at 5000 rpm both the ends of disc were broken which was the first success, a mile stone towards the validation, experimental test rig. Specimen showing the area from which disc was broken is given in Figure 11.



Figure 11. Specimen showing the area from which disc was broken.

The specimen of disc was produced from structural steel by using the wire cutting machine with the same dimensions and tried out starting from zero rpm and when it reached at 14000 rpm disc was broken without damaging the testing system as well as operator. This has not only evaluated the experimental testing system but also confirmed the safeties introduced. Specimen showing the area from which disc was broken is given in Figure 12.

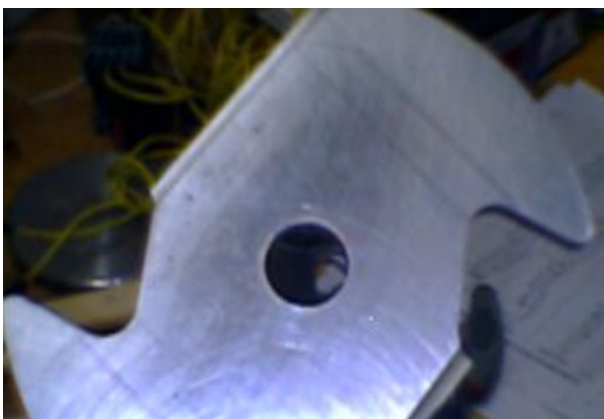


Figure 12. Specimen showing the area from which disc was broken.

3. Numerical Simulation

Element size of one is used in the analysis as shown in Figure 13, because further reducing the size of element increases the computational time exponentially. After performing the initial analysis, local meshing was performed in critical areas as given in Figure 14 for precise results. The gravitational effect and cylindrical frictional support is added in the model as boundary conditions. To calculate stress/strain and estimate the fatigue life of the model, rotational velocity applied to the model was increased from zero to a maximum value in steps, each step is of size 100 rpm in five seconds.

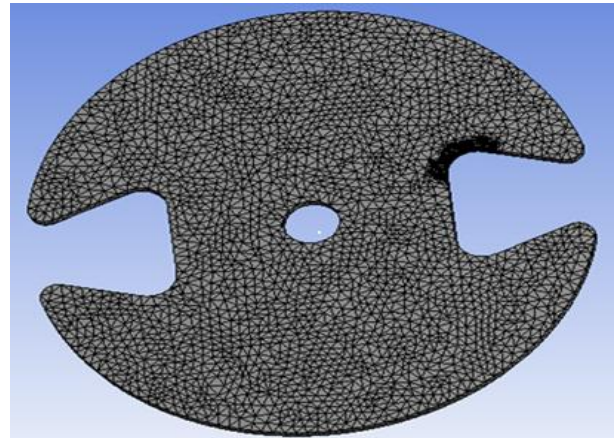


Figure 13. The model of disc after meshing

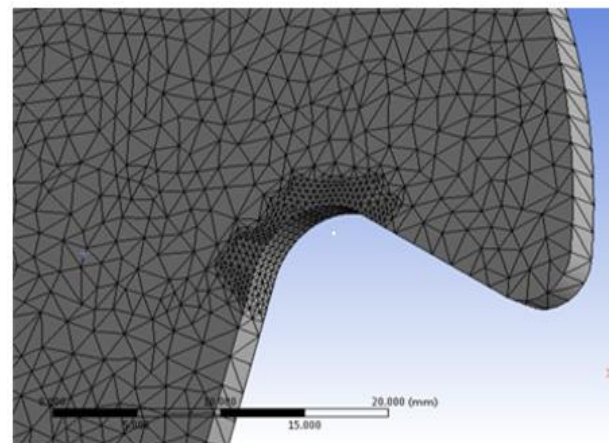


Figure 14. The enlarged view of model of disc after meshing in critical region.

After initial analysis, it was found that the fillet spot area is the weakest link in the model where the failure due to fatigue initiates. The number of

nodes in the critical region was different depending on the meshing size as the meshing size were changed to a finer value at different stages to have more precise results. To optimize the fatigue life, different materials and geometrical shapes were analyzed and then results were compared with the experimental results. Five points were marked as shown in Figure 15 on the surface of fillet to investigate the point of interest where the highest stress/strain was developed.

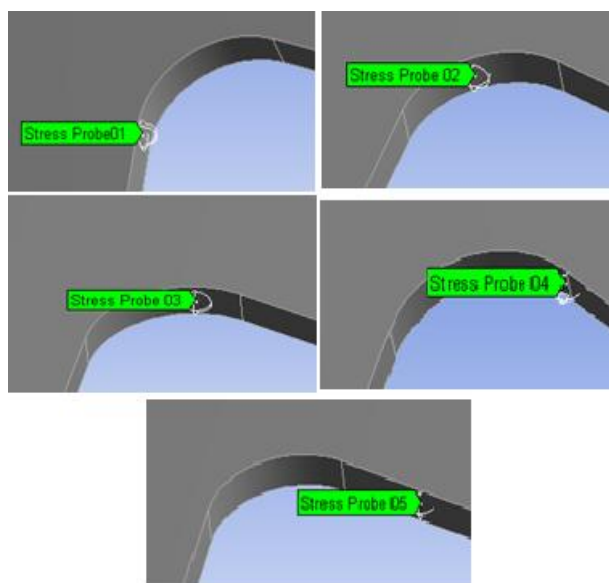


Figure 15. The stress probe 1,2,3,4 and 5 on the fillet surface of the disc.

Stress Probe 1 and 4 are on the edges of fillet and stress Probe 2 and 3 are between the stress Probe 1 and 4 as we proceed from stress Probe 1 to 4, and stress Probe 5 is away from stress Probe 4 towards the end of disk.

4. Results and Discussion

This research work has been performed experimentally and computed numerically the fretting fatigue crack initiation in dovetail joint for aero engine compressor by using newly developed experimental fretting fatigue test rig and three dimensional finite elements analysis through commercially available software respectively.

Different type of fretting fatigue, experimental testing rigs were developed by researchers to evaluate the fretting fatigue phenomenon in the disc & blades assembly fixed in dovetail joint of an aero engine compressor. Pauw et al. [21]

concluded that researchers use the existing rigs as such or with certain modification or develop new testing rigs to fulfill their requirement but still no standard and generally acceptable testing rig is available for fretting fatigue experimental. Results of any two type of testing rigs hardly match with each other.

A new test rig was designed and developed with additional features revolving the actual geometry of the specimen in a sinusoidal wave. Verification of the rig was carried out with & without specimen which has already been discussed in para 2.5. Experiment was performed at room temperature and material used was bakelite and structural steel. In case of structural steel specimen remained in revolving condition in the range of 0 ~20,000 rpm and after 100 cycles no failure was observed. The specimen was removed from the testing rig and examination was carried out critically and found dark band on the contact surfaces of disc and blade which was expected and has already been investigated by many researchers.

Both the specimens made of bakelite & structural steel were rotated in the range of 0~20,000 rpm and disc made of bakelite material was broken at 5,000 rpm whereas structural steel was broken at 14,000 rpm from the expected weakest portion of the fillet which has already been concluded by various researchers through experimentally as well as numerically.

Comparison of stresses at these five points shows stress variation as we move from inner edge of the fillet toward the end of the disk. Although the equivalent stress is greater than the shear stress, but shear strain is greater than the normal strain, which clearly indicates that the failure is due to shearing. The shear strain due to the shear stresses is highest as compared to the other types of stresses; shows that the failure is based on maximum shear theory. The maximum shear stress variation at stress probe 4 is given in Figure 16 and Shear stress variation at stress Probe 1~ 5 is given in Table 3, whereas trend has been shown in Figure 17. The maximum principal stress at stress probe 4 is given in Figure 18 and maximum Principal Stress variation at stress Probe 1~ 7 is given in Table 4, whereas trend has been shown in Figure 19.

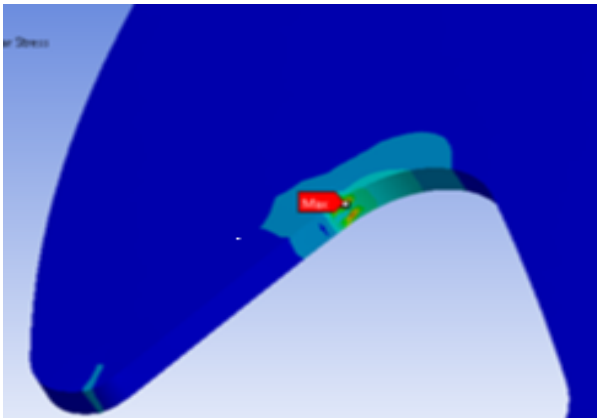


Figure 16. Maximum shear stress at stress probe 4.

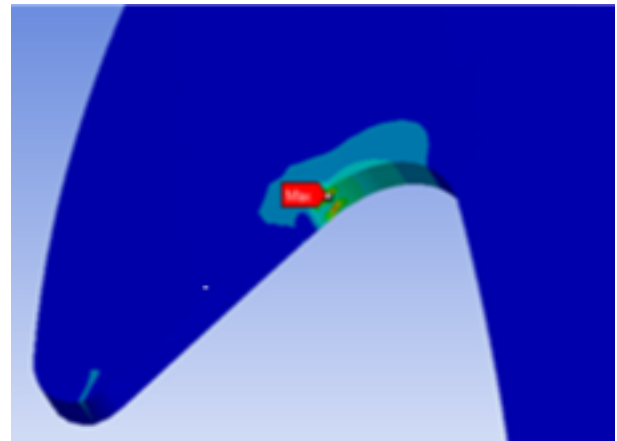


Figure 18. Maximum principal shear stress at stress probe 4.

Table 3. Stress variation at stress PProbes 1~7.

| Object Name | XZ Shear | YZ Shear | XZ Shear |
|----------------|----------|----------|----------|
| Stress point 1 | 0.00 | 0.00 | 0.13 |
| Stress point 2 | 0.07 | 0.00 | 0.02 |
| Stress point 3 | 0.12 | 0.00 | 0.02 |
| Stress point 4 | 0.25 | 0.07 | 22.57 |
| Stress point 5 | 0.15 | 0.05 | 19.0 |
| Stress point 6 | 0.05 | 0.03 | 13.0 |
| Stress point 7 | 0.01 | 0.02 | 7.46 |

Table 4. Principal Stress variation at stress PProbes 1~7.

| Object Name | Equivalen (von-Mises) | Maximum Principal | Middle Principal | Minimum Principal |
|----------------|-----------------------|-------------------|------------------|-------------------|
| Stress point 1 | 4.63 | 0.00 | 0.00 | 0.00 |
| Stress point 2 | 31.34 | 31.40 | 0.07 | 0.06 |
| Stress point 3 | 49.66 | 49.63 | 0.02 | 0.00 |
| Stress point 4 | 74.10 | 87.66 | 17.56 | 10.12 |
| Stress point 5 | 77.09 | 82.54 | 15.56 | 9.19 |
| Stress point 6 | 55.14 | 60.24 | 5.10 | 5.1 |
| Stress point 7 | 13.04 | 8.42 | 0.00 | -0.05 |

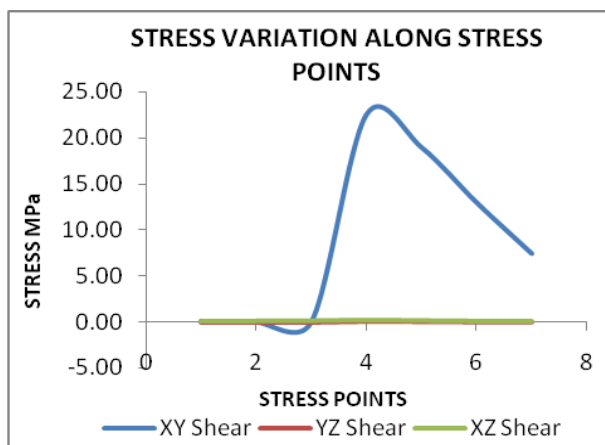


Figure 17. Trend of shear stress variation at stress probes 1~7.

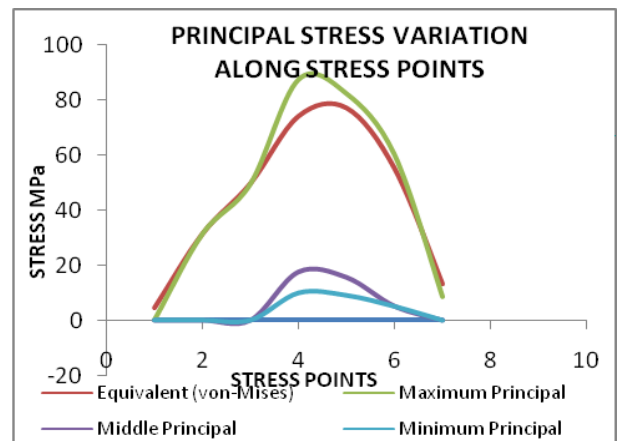


Figure 19. Trend of principal shear stress variation at stress probes 1~7.

From Table 3 and Figure 17 it is shown that shear stress at stress point 4 along XZ, YZ and XY plan is 0.25, 0.07 and 22.57 MPa respectively which is highest as compared to the other stress

point 1, 2, 3, 5,6 and 7 whereas in Table 4 and Figure 19 principal stresses value at stress point 4 is 10.12, 17.56, 87.66 and 74.1MPa which has the maximum values as compared to other stress points 1, 2, 3 , 5, 6 and 7.

The exact node numbers from where failure/shear initiates, can also be found, but not given here because of mesh refinement at different stages. Points along the fillet are provided with stresses to find exact location of failure initiation. The point of maximum stress is about 3-4 the distance between inner edges and the outer edge of fillet, when moving along the inner

To optimize the design, a number of iterations were performed with different materials and thickness of the disk. Irrespective of the material and thickness of the disk, each iteration analysis shows that the fillet is the weakest link in model as shown in Figure 20.

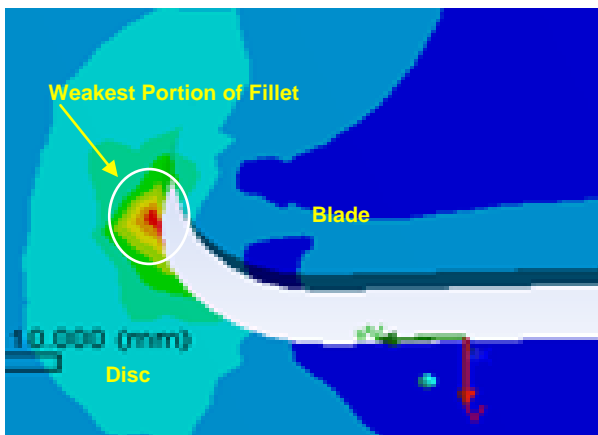


Figure 20. Maximum principal stress at stress probe 4 (crack initiation tip).

By changing the material or thickness of the disk failure initiation located do not change, only the fatigue life is affected that is same as in the prototype testing.

5. Benchmarking of Apparatus

Based upon the experimental analysis and simulation on same geometrical / material model we can safely benchmark for crack and fretting fatigue studies.

6. Conclusion

This research paper designed a unique, flexible, safe and improved fretting fatigue experimental test

rig to study disc and blades assembled in dove tail joint of aero engine compressors. Experimental test rig has the capability to revolve actual geometry in sinusoidal wave which is the actual simulation of aero engine compressors. Many conclusions can be made from the initial test, which have been performed with the newly developed test rig.

- a. Dark band having black powder found on the sliding surfaces causes the crack initiation development.
- b. In three-dimensional finite elements analysis it was concluded that fillet was the weakest portion of the dovetail joint disc for both the cases irrespective of the thickness and type of material.
- c. When the material fracture takes place the working life changes with the change of rpm.
- d. Fatigue cracks develop in the region of tension rather than compression.
- e. By changing the disk material fatigue life changes.
- f. With the change of disk thickness fatigue life changes.

Acknowledgements

We are indebted to the University of Engineering and Technology Taxila Pakistan, National University of Sciences and Technology Pakistan, for acquiring research material for this study. We are also thankful to Pakistan Science Foundation (PSF) and Higher Education Commission (HEC) for providing assistance.

References

- [1] Conner, Lindley, Nicholas and Suresh International Journal of Fatigue **26** (2004) 511.
- [2] Eden and Rose, Proceedings of the Institute for Mech Engineers **4** (1911) 839.
- [3] Tomilson, Proceedings of the Royal Society, London, Series A **115** (1927) 472.
- [4] Nowell, Doctor of Philosophy Thesis, Lincoln College, Oxford University (1988).
- [5] Shinde and Hoepfner, Wear **259** (2005) 271.
- [6] Alfredsson and Cadario, International Journal of Fatigue **26** (2004) 1037.

- [7] Conner, Hutson and Chambonc, *Wear* **255** (2003) 259.
- [8] Nowell and Dini, *Tribology Int.* **36** (2003) 71.
- [9] Ramakrishna and Ganesh, *International Journal of Fatigue* **27** (2005) 663.
- [10] Fouvry, Duo and Perruchaut, *Wear* **257** (2004) 916.
- [11] Hutson, Neslen and Nicholas, *Tribology Int.* **36** (2003) 133.
- [12] Smith, Watson and Topper, *J. Mater* **5**, (1970) 767.
- [13] Namjoshi, Shantanu, Mall, Jain and Jin, *Fatigue Fracture Eng. Mater. Struct.* **25** (2002) 955.
- [14] Findley, *ASME. J. Eng. Ind.* **B81** (1959) 301.
- [15] Hammouda, Pasha and Fayad, *International Journal of Fatigue* **29** (2007) 30.
- [16] Malay, Mahendra and Madan, *SAS Tech.* **8**, No. 1 (2009) 71.
- [17] Kaliyaperumal, Raghu, Prakash and Antonio, *World Academy of Science, Engineering and Technology* **46** (2010) 879.
- [18] Tiago, Gustavo and Joao, *Instituto Tecnológico de Aeronautica-SAO Jose dos Campos/SP-Brazil* (2012) 51.
- [19] Patrick and Golden, *International Journal of Fatigue* **31** (2009) 620.
- [20] Borms, Schamphelaere, Pauw, Baets and Waele, Ghent University, Laboratory Soete, Belgium. *Sustainable Construction and Design* (2011) 370.
- [21] Pauw, Baets and Waele, Ghent University, Laboratory Soete, Belgium. *Sustainable Construction and Design* (2011) 41.